ELSEVIER
Available online at www.sciencedirect.com
ScienceDirect
Procedia CIRP 48 (2016) 236 – 241
www.elsevier.com/locate/procedia

23rd CIRP Conference on Life Cycle Engineering

Stochastic Tool Wear Prediction for Sustainable Manufacturing

Peng Wang and Robert X. Gao*

Department of Mechanical and Aerospace Engineering, Case Western Reserve University, Cleveland, OH 44016, USA

* *Tel.*: +1-216-368-6045; *fax*: +1-216-368-6445; *E-mail address:* Robert.Gao@case.edu

Abstract

To provide scientific support for decision-making in critical applications such as maintenance scheduling and inventory management, tool wear monitoring and service life prediction are of significance to achieving sustainable manufacturing. Past research typically assumed time-invariant machining settings in modeling wear progression, hence is limited in accurately tracking varying wear rates. This paper presents a stochastic joint-state-and-parameter model with machining setting as a parameter that affects the state evolution or tool wear propagation. The model is embedded in a particle filter for recursive wear state prediction. Effectiveness of this method is verified through experimental data measured on a CNC milling machine.

Peer-review under responsibility of the scientific committee of the 23rd CIRP Conference on Life Cycle Engineering

Keywords: Tool wear prediction; stochastic modeling; particle filter

1. Introduction

Sustainable manufacturing purses environmental and societal safety besides economic benefit [1]. Specifically, the goals of sustainable manufacturing are improving manufacturing efficiency, extending product life, reducing energy and resource improvement, minimizing toxic waste and occupational hazards. Machine tool should play an important role in achieving the sustainable manufacturing, since it has an almost 100 billion consumptions each year [2].

The post-use of machining tool can significantly reduce material consumption and increase economic benefit, through regenerating of retired tools, by recover, recycle, redesign based on former performance, remanufacture and redesign [3], as shown in Fig. 1. Advanced monitoring of machining tool wear progression and understanding its underlying physical nature can benefit:

- Predicting accurately the tool remaining useful life of tool, reducing the cost due to additional downtime and unscheduled maintenance;
- Optimizing machining planning, finding optimal machining settings that can increase extend tool life and increase manufacturing efficiency.

Past researches indicated that the tool wear propagation would vary with different machining settings (e.g. cutting speed, feed rate, cut depth and workpiece material). As an example shown in Fig. 2, the relationship between tool wear rate and feed rate under certain cutting speed (in symbol v) and depth is quadratic, which means an optimal feed rate exists for longest tool life. In this paper the physics-based wear modelling with respect to machining settings is focused, through which it is expected to optimize operating scheduling.

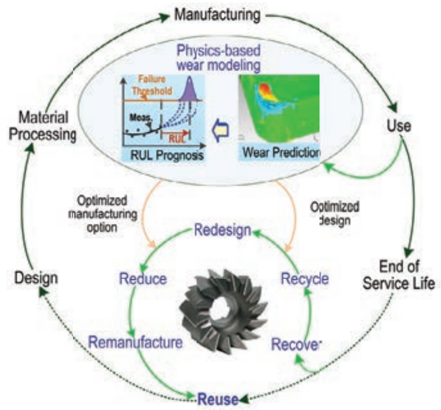

Fig. 1 life cycles of machining tool in sustainable manufacturing

Peer-review under responsibility of the scientific committee of the 23rd CIRP Conference on Life Cycle Engineering
doi:10.1016/j.procir.2016.03.101

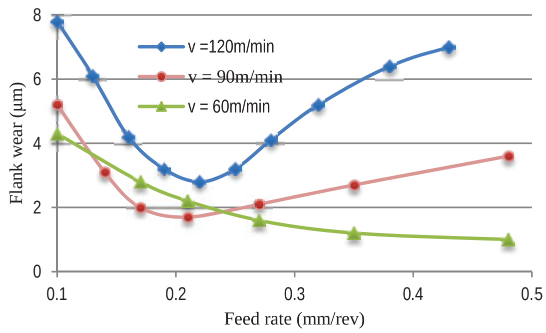

Fig. 2 Effect of feed rate on tool flank wear [4]

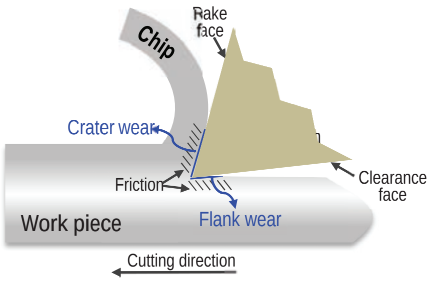

Fig. 3 Mechanism for friction and tool wear

Most studies on wear mechanism numerically establish relationships between propagation of tool wear (width, measured by microscope) and machining settings and material prosperities, and label/determine the coefficients in the equations with large amount of experimental data [5]. For example, a generalized form of extended Taylor's law is presented to predict the tool life as a function of cutting parameters and workpiece hardness [6]. Different mechanisms, such as abrasion (Fig. 3), adhesion and diffusion are investigated to describe tool wear rate under different machining settings and materials [7]. Additional factors, such as the geometry of tool [8] and cutting temperature [9], have also been investigated. Since no derived equations can exhaust the physical nature of tool wear, labelled parameters based on the experimental data would vary with different machining situations. Under this scenario, parameters need to be iteratively calibrated, which is time-consuming and therefore not practicable.

The other approach, instead, employs observable sensor measurement (e.g. current, force, vibration, and acoustic emission) to infer the wear status and determine the wear model without interrupting the machining process. The inference can be achieved by a model-based approach, which embeds the analytical models representing the dynamic process (e.g. tool wear) in a filtering (e.g. Kalman filter or particle filter). It can account for the stochasticity of the process and noise embedded in the measurement [10], providing more explanation on the prediction results. Compared to Kalman filter, particle filter (PF) has no Gaussian assumption and stronger capability to describe a non-linear system [11], thus it is investigated as the main technique in this paper.

To achieve the goal that directly determine the tool wear growth with respect to machining settings in the manufacturing process, this paper a stochastic joint-state-and-parameter estimation framework based on PF with machining settings as parameters that affects the tool wear propagation, based on past work [12]. One state evolution model describing wear progression and one measurement model describing relationship between wear and sensor measurements are defined under the framework. Coefficients in these two models are assumed to vary with machining settings and estimated by an improved particle filter (PF), which can achieve better estimation accuracy with fewer particles through an adaptive resampling strategy.

2. Particle filter based prediction

A dynamic system can be estimated through Bayesian inference with a state model and a measurement model. The state model describes the evolution of the state (variables x representing tool wear in this paper) over time, which is conditionally based on machining settings D (e.g. spindle speed, feed rate, cutting depth, material prosperity) and parameters θ (or coefficients, describing the effects of setting factors) θ and process noise w which denotes the randomness of tool wear propagation and wear modelling error.

$$x_k = f_k\left(x_{k-1}, D_k, \theta_k, w_k\right) \tag{1}$$

where f_k describes the state transition function from state x_{k-1} to x_k considering an order-one Markov process [13]. The discrete sampling time is denoted by k. The measurement model, describe the relationship between sensor measurement and machining settings and wear severity is given by:

$$z_k = h_k\left(x_k, D_k, \phi_k, v_k\right) \tag{2}$$

where h_k is the measurement function representing the relation between observable sensor output z_k and an unobservable degradation state x_k. $_k$ denotes the effects of the machining settings in the measurement model. Measurement noise caused by environmental noise and/or limitations of sensors is denoted by v_k. Generally, both state and measurement models are nonlinear in practical applications. The estimation of x_k given available information of measurement z_k and machining setting D_k can be achieved through calculating the posterior probability density function (pdf) $p(x_k|z_k)$ via Bayesian inference through two steps: prediction and update, as illustrated in (3) and (4).

$$\begin{aligned} p\left(x_k, \theta_k, \phi_k \mid z_{k-1}, D_k\right) = \int p\left(x_k, \theta_k, \phi_k \mid x_{k-1}, \theta_{k-1}, \phi_{k-1}, D_k\right) \\ p\left(x_{k-1}, \theta_{k-1}, \phi_{k-1} \mid z_{k-1}\right) dx_{k-1}\theta_{k-1}\phi_{k-1} \end{aligned} \tag{3}$$

$$\begin{aligned} p(x_k, \theta_k, \phi_k \mid z_k, D_k) &= \frac{p(z_k \mid x_k, \theta_k, \phi_k)\, p(x_k, \theta_k, \phi_k \mid z_{k-1})}{p(z_k \mid z_{k-1}, D_k)} \\ &= \frac{p(z_k \mid x_k, \theta_k, \phi_k)\, p(x_k, \theta_k, \phi_k \mid x_{k-1}, \theta_{k-1}, \phi_{k-1}, D_k)\, p(x_{k-1}, \theta_{k-1}, \phi_{k-1} \mid z_{k-1})}{p(z_k \mid z_{k-1}, D_k)} \end{aligned} \tag{4}$$

where $p(z_k|z_{k-1})$ is can be calculated as:

$$p(z_k \mid z_{k-1}, D_k) = \int p(x_k, \theta_k, \phi_k \mid z_{k-1}, D_k)\, p(z_k \mid x_k, \theta_k, \phi_k)\, dx_k \theta_k \phi_k \tag{5}$$

Equation (3) employs the measurement in the last sampling time to predict the tool wear at current moment, which is then corrected by current measurement. It can be seen from (3) that unknown parameters θ_k and ϕ_k are derived upon both the historical measurement and machining setting D, which means the parameters would vary with different machining settings. Hence, the objective of modeling wear progression considering time-variant machining settings can be achieved. Equations (3) and (4) translate the problem of posterior pdf estimation into the calculation of likelihood function $p(z_k|x_k, \theta_k, \phi_k)$ and prior distribution $p(x_k, \theta_k, \phi_k|x_{k-1}, \theta_{k-1}, \phi_{k-1})$. But an exact solution for (3) and (5) is usually intractable, due to the difficulty in calculating the integral especially when the state and measurement are described in high-dimensional space.

The PF algorithm, based on Monte Carlo method, employs a set of random samples/particles $\{x_k^i, \theta_k^i, \phi_k^i$, i = 1, 2, …, $N\}$ and associated importance weights w_k^i to provide an approximated solution to the posterior pdf. The integral operation in (3) is approximated as the summation of these weighted random numbers as:

$$
\begin{aligned}
&p(x_k,\theta_k,\phi_k \mid z_{k-1}) \\
&\approx \sum_{i=1}^{N} w_{k-1}^i \delta\Big((x_k,\theta_k,\phi_k)-(x_{k-1}^i,\theta_{k-1}^i,\phi_{k-1}^i)\Big) p(x_k,\theta_k,\phi_k \mid x_{k-1},\theta_{k-1},\phi_{k-1}) \\
&= \sum_{i=1}^{N} w_{k-1}^i p(x_k,\theta_k,\phi_k \mid x_{k-1}^i,\theta_{k-1}^i,\phi_{k-1}^i)
\end{aligned} \tag{6}
$$

Equation (6) indicates that the estimation of the posterior pdf relies on a predefined prior pdf $p(x_k,\theta_k,\phi_k \mid x_{k-1}^i,\theta_{k-1}^i,\phi_{k-1}^i)$, where particles are sampled initially, as the example shown in Fig. 4, where the circle and its size denote the particle and weight. The mapping from the prior pdf to the posterior pdf is regulated by the weights of particles. The adjustment of the weights is upon the new measurement, by calculating the likelihood of it given the predicted state from (6)

$$
w_k^i \propto w_{k-1}^i p(z_k, \mid x_k^i, \phi_k^i, D_k) \tag{7}
$$

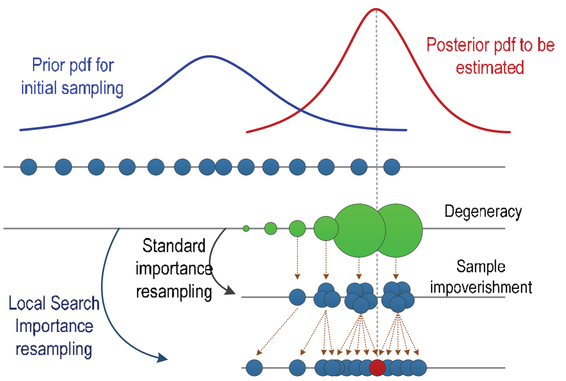

Fig. 4 Sampling, conventional resampling and enhanced adaptive resampling (circles represent the particles; positions of circles represent the estimated values of states and/or parameters; and dimensions of circles represent the weights of particles)

An inherent problem of the above algorithm is particle degeneracy, which means after several iterations most of the computational load is wasted on the updating of particles with negligible contribution to the state update. A popular solution is importance resampling that removes particles with small weights (by comparing normalized weight to a predefined number within 0~1) and retains particles with large weights. However, this process introduces the particle impoverishment problem that the number of unique particles decreases greatly. These two problems are actually caused by the fact that the positions of particles sampled from the initial prior distribution are fixed throughout the estimation process [14], as described in Fig. 4. This also obstructs conventional PF on tracking a dynamic system with varying degradation rate. In addition, the estimation accuracy of posterior pdf can be greatly affected by the quality of initially selected prior pdf.

To tackle the particle degeneracy and sample impoverishment problems associated with standard particle filter, the resampling strategy needs to be changed from discrete approximation to continuous approximation, while maintaining a balance between keeping particle diversity (a degree to quantify unique and active particles) and ensuring particles' tracking performance (diverse particles may increase the confidence interval of the estimation, leading to reduced estimation accuracy). This can be done through dispersing the particles with large weights in the resampling process from fixed positions to a wider range by adding a perturbation to each particle [15]. The perturbation for each particle is sampled from a normal distribution, which is determined by their estimation accuracy in the last iteration step:

$$
p\left(\theta_{k+1}^i \mid \theta_k^{r(l)}\right) \propto N\left(\theta_{k+1}^i \mid \theta_k^{r(l)}, hP_k^{r(l)}\right) \tag{8}
$$

where P represent the variance of particles' estimations:

$$
P_k^{r(l)} = E\left[\left(\theta_k^{r(l)} - \frac{1}{N}\sum_{i=1}^{N} w_k^i \theta_k^i\right)\left(\theta_k^{r(l)} - \frac{1}{N}\sum_{i=1}^{N} w_k^i \theta_k^i\right)^T\right] \tag{9}
$$

where

$$
r(l): \left\{\sum_{i=1}^{l} w_k^j \geq rand\right\} \tag{10}
$$

represents the selected ith particle at iteration k+1 from iteration k and $\frac{1}{N}\sum_{i=1}^{N} w_k^i \theta_k^i$ adopted as the best estimation at iteration k to determine each particle's estimation accuracy. $P_k^{r(l)}$ represents the variance of the normal distribution, from which a perturbation is generated for the ith particle at iteration k+1. The symbol h denotes the shrinkage coefficient, which decreases through the iteration process, to ensure convergence of estimation by PF.

A particle associated with a larger weight will be assigned with a smaller search range when entering into the next iteration, due to its being closer to the relatively best estimation. Otherwise, a particle is assigned with a larger search range. Dispersing samples not only increases the number of unique and active particles, but also causes particles in the subsequent iterations to move to the global optimal solution (represented by the grey dash line in Fig. 4) continuously. Consequently, the final estimation result eliminates mismatch between the prior pdf and posterior pdf.

The decreasing shrinkage coefficient ensures samples to gradually converge to the optimal location, consequently narrowing down the confidence interval and provide more accurate prediction.

3. Tool wear rate models

3.1Tool wear evolution model

Common types of wear include frank wear and crater wear, which are subjected to the abrasive or adhesive interaction between tool and workpiece, as shown in Fig. 3. Frank wear length is mainly investigated in this paper, since it is generally regarded as the tool life criterion to evaluate tool performance [7]. Tool wear propagation can be treated as a specific type of crack growth, and hence can be modeled based upon Paris' law.

$$\frac{dx}{dt} = cx^m \tag{11}$$

Here, parameters c and m only consider the effect of machining materials. To include other machining settings, such as spindle speed, feed rate f, cutting depth d, (10) can be modified as:

$$\frac{dx}{dt} = f^A d^B x^C \tag{12}$$

Coefficient A and B represent the effects of f and d on wear progression. Expression of wear x as a function of time can be obtained through integrating (11):

$$x = \left[f^A d^B (1-C) t \right]^{\frac{1}{1-C}} \tag{13}$$

A discretized version of (12) is:

$$x_k = \left[x_{k-1}^{1-C} + f^A d^B (1-C)(t_k - t_{k-1}) \right]^{\frac{1}{1-C}} \tag{14}$$

One example demonstrating the effect of feed rate and cutting depth is shown in Fig. 5. It indicates the tool wear rate decreases with the decrease of the feed rate and cutting depth, and cutting depth influences more than feed rate. The influences of machining setting factors would be reflected in estimated coefficients/parameters A and B. It should be noted in this paper that these parameters are assumed to be constant under same machining setting.

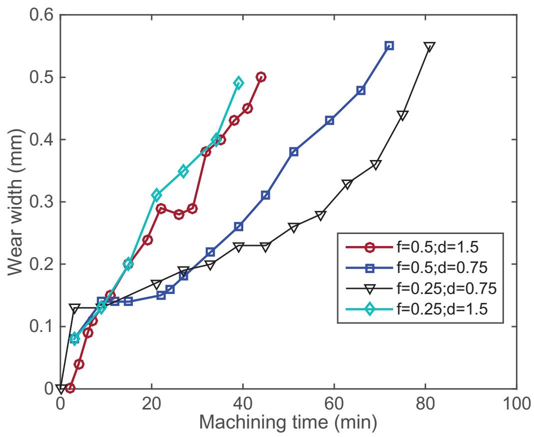

Fig. 5 Tool wear propagation with respect to machining settings

3.2 Measurement model

Typical measurements applied to tool wear monitoring include force, vibration, current and acoustic emission. For measurement such as force and power that can be derived with an explicit function with respect to wear, the measurement model can directly utilize the function. For example, the relationship between cutting force and wear under the effect of machining settings can be described as [16]:

$$Force = Ef^E d^G + Hx \tag{15}$$

where E, F, and G are the coefficient need to be estimated by PF. For other measurement, such as vibration and acoustic emission, feature extraction based on Kullback-Leibler (KL) divergence is investigated, by fully taking advantage of the fact that all measurements within one cut can be seen as a distribution [15]. It is assumed that the distribution shifts when tool wear deteriorates. Thus the distance between two distributions can be seen as an indicator to reveal the wear. Let $p_1(x)$ and $p_2(x)$ be two distributions, the information of KL divergence from p1 to p2 is defined as:

$$KL(p_1, p_2) = \int p_1(x) \frac{p_1(x)}{p_2(x)} dx \tag{16}$$

Smaller values of the information quantity $KL(p_1, p_2)$ mean that the distance between two distributions is smaller. That is, the larger the distance between two distributions, the larger the difference between two distributions. In this paper, the distribution obtained from the initial time is taken as the reference distribution, and the new distribution is compared to the reference distribution to calculate the KL information, which is subsequently applied to estimate the tool wear. Due to quite the complex mechanisms of both tool wear and force or vibration measurement, it is difficult to establish definite relationship between wear and extracted KL information. The relationship can be obtained an empirical model:

$$KL = Df^E d^F x^G \tag{17}$$

Therefore, there are seven parameters A~G to be estimated by PF. It should be noted the initial value of these parameters are obtained through a rough guess based on prior knowledge, and the initialization would not affect the estimation result much by the proposed PF.

4. Experimental evaluation

To evaluate the performance of proposed tool wear prediction method, data taken from a Matsuura milling machine MC-510V under different machining settings are processed and estimated. The Experimental setup and data acquisition are shown in Fig. 6. Data sampled by five different sensors, two acoustic emission sensor (one on table, one on the spindle), two vibration sensors and one current sensor are installed to determine the state of tool wear [17]. The evolution of acoustic emission data with respect to different wear severity is shown in Fig. 7 as an example. Two sets of data under four different machining settings (as shown in Table 1, and their effects on tool wear progression shown in Fig. 5) are investigated in this paper, with one used for training process to estimate the parameters in (13) and the other one to predict tool wear and testify the effectiveness of the proposed method.

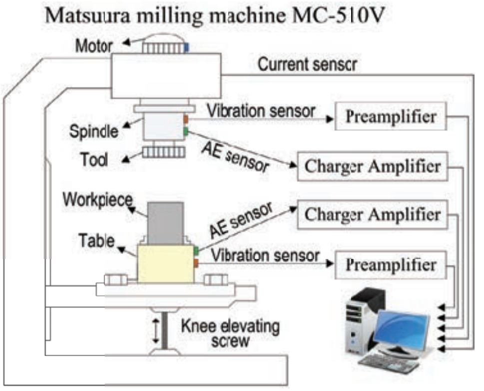

Fig. 6 Experimental setup and data acquisition

Table 1. Design of experiments

	Cutting speed (m/min)	Cutting depth (mm)	Feed rate (mm/rev)
Case 1	200 m/min	1.5	0.5
Case 2		0.75	0.5
Case 3		0.75	0.25
Case 4		1.5	0.25

Initially, the unknown parameter pair *A~G* are modeled as probability distributions following a certain distribution (e.g. uniform distribution in this paper). The initial distribution selection can determine the performance of standard PF, but not improved PF proposed in this paper. In the learning stage, based on the state model (13) and measurement models (14) and/or (16), the unknown parameters *A~G* can be estimated recursively and obtained as a priori. The latest updated parameters *A~C* under different machining settings would be used for prediction. It should be noted in this paper that the machining settings are assumed to be known in advance, and the parameters representing the effect and machining factors on tool wear progression are assumed to maintain constant under same machining settings. Fig. 8 shows the predicted tool wear for different cutting depths. The black box in the figure represents the interquartile range (50% confidence range) of the prediction.

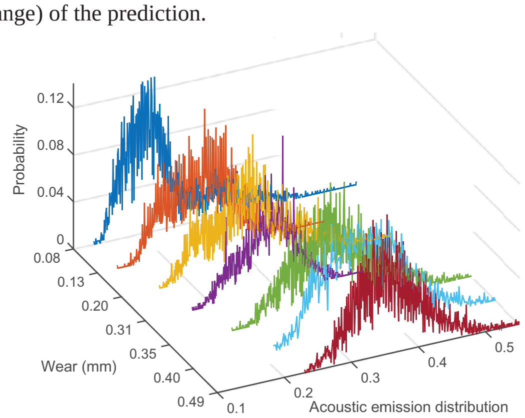

Fig. 7 Distributions of acoustic emission for different wear levels

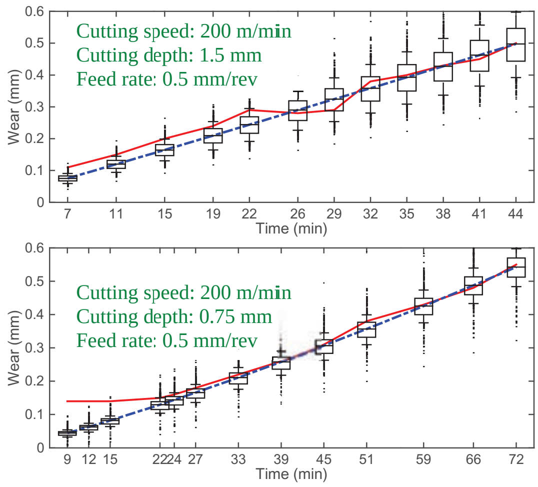

Fig. 8 Tool wear prediction for different cutting depths

Figure 9 shows the evolution of parameter estimation for Case 2, with the blue lines as median estimations and red lines as 90% confidence limits of estimations. It can be noted that the estimated parameters' distributions concentrate on smaller ranges (i.e. the width between two red lines) continuously, which is the advantage of proposed PF over standard PF.

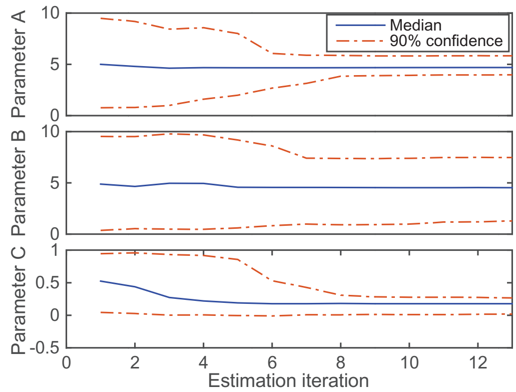

Fig. 9 Evolution of estimated parameters in state evolution model

Since PF is an estimation method based on random sampling, the stability and robustness of the algorithm should be demonstrated. Results of Monte Carlo simulations are shown in Fig. 10. Each case has been run for 100 times. Both the median (blue line) of the predictions and error bars are shown in the figure. Both Fig. 8 and Fig. 10 demonstrate the tool wear predictions for different machining settings based on improved PF are accurate and robust.

Estimated parameters for different machining settings based on the train data by improved PF are shown in Table 2. When the planned machining settings are known, the future tool wear can then be predicted. Fig. 11 shows tool wear prediction for varying machining settings, in which tool undergo different wear rate under phase 1 and phase 2. The results demonstrate the proposed method, in which machining setting factors are modeled as parameters in the state evolution model and measurement model, and then estimated by improved PF and used for prediction, is effective.

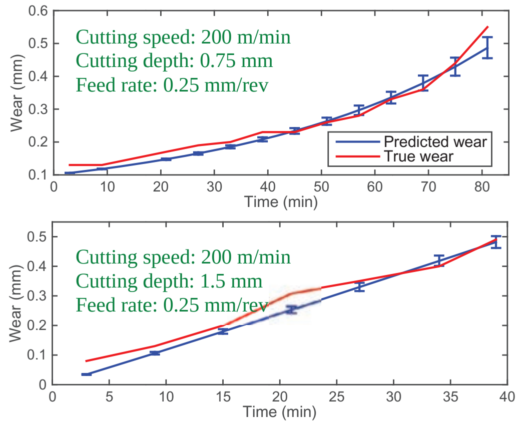

Fig. 10 Tool wear prediction for different feeding rates

Table 2 Estimated parameters by particle filter

Case	f	d	Parameter A	Parameter B
1	0.5	1.5	4.8867	-2.2227
2	0.5	0.75	4.7073	4.6192
3	0.25	0.75	1.7151	4.4621
4	0.25	1.5	1.6469	-7.7653

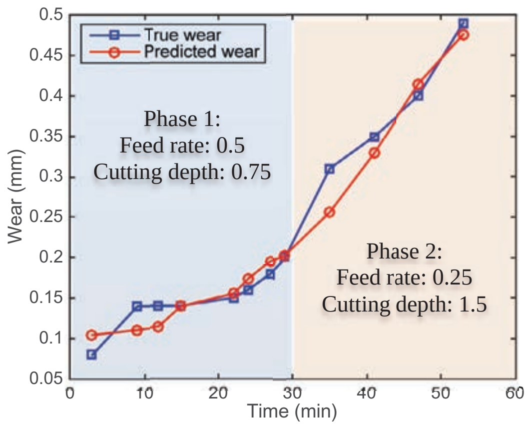

Fig. 11 Tool wear prediction for varying machining settings

Through Monte-Carlo simulation tests, the improved PF has demonstrated its ability on accurately determining the effects of machining settings on tool wear propagation and precisely predict the tool wear. The determination of effect of machining settings can subsequently be used to finding the optimal machining settings online.

Conclusions

A Particle Filtering enabled join-state-and-parameter estimation and prediction framework has been proposed with the prediction of the severity of tool wear under different machining settings as an example. Machining settings have been taken as unknown parameters in the state evolution model and measurement model into consideration, to account for more robust and reliable prediction. The estimated parameters and state evolution model can then be utilized to predict tool wear when the machining settings are known. Aiming at the sample impoverishment problem, an improved version of PF has been proposed through refining the resampling strategy. With the performance evaluated by a tool wear test in a CNC milling machine, the proposed method is demonstrated to accurately and robustly determine the effect of machine settings and predict the tool wear growth, while the letter can be used to optimize the machining scheduling.

Acknowledgements

This research has been partially supported by National Science Foundation under grant CCF-1331850 and CMMI-1300999.

References

[1] Yuan C, Zhai Q, Dornfeld D. A three dimensional system approach for environmentally sustainable manufacturing. CIRP Annals - Manufacturing Technology 2012; 61(1): 39-42.

[2] Gardner, 2015 world machine tool output and consumption survey, 2015.

[3] Jayal AD, Badurdeen F, Dillon OW, Jawahir IS. Sustainable manufacturing: modeling and optimization challenges at the product, process and system levels. CIRP Journal of Manufacturing Science and Technology 2010; 2: 144-152.

[4] Astakhov VP. Effects of the cutting feed, depth of cut, and workpiece (bore) diameter on the tool wear rate. The International Journal of Advanced Manufacturing Technology 2007; 34(7-8): 631-640.

[5] Li B. A review of tool wear estimation using theoretical analysis and numerical simulation technologies. International Journal of Refractory Metals and Hard Materials 2012; 35: 143-151.

[6] Poulachon G, Moisan A, Jawhir IS. Tool-wear mechanisms in hard turning with polycrystalline cubic boron nitride tools. Wear 2001; 250(1-12): 576-586.

[7] Huang Y, Liang S. Modeling of CBN tool flank wear progression in finish hard turning. Transactions of ASME 2004; 126: 98-106.

[8] Karpuschewski B, Schmidt K, Beno J, Mankova I, Frohumller R, Prilukova J. An approach to the microscopic study of wear mechanism during hard turning with coated ceramics. Wear 2015; 342-343: 222-233.

[9] Luo X, Cheng K, Holt R, Liu X. Modeling flank wear of carbide tool insert in metal cutting. Wear 2005; 259: 1235-1240.

[10] Baraldi P, Mangili F, Zio E. Investigation of uncertainty treatment capability of model-based and data-driven prognostic methods using simulated data. Reliability Engineering and System Safety 2013; 112: 94-108.

[11] Wang J, Wang P, Gao R. Enhanced Particle Filter for Tool Wear Prediction. Journal of Manufacturing Systems 2015; 36: 35-45.

[12] Gao R. Wang L, Teti R, Dornfeld D, Kumara S, Mori M, Helu M. Cloud-enabled prognosis for manufacturing. CIRP Annals-Manufacturing Technology 2015; 64(2):749-772.

[13] Arulampalam MS, Maskell S, Gordon N, Clapp T. A Tutorial on particle filters for online nonlinear/non-gaussian bayesian tracking. IEEE Transactions on Signal Processing 2002; 50(2): 174-188.

[14] Li T, Sun S, Sattar T, Corchado J. Fight Sample Degeneracy and Impoverishment in Particle Filters: A Review of Intelligent Approache. Expert Systems with Application 2014; 51: 3944-3954.

[15] Wang P, Gao R. Adaptive Resampling-Based Particle Filtering For Tool Life Prediction. Journal of Manufacturing Systems 2015; 37(2): 528-534.

[16] Shao H, Wang H, Zhao X. A cutting power model for tool wear monitoring in milling. International Journal of Machine Tool and Manufacture 2004; 44: 1503-1509.

[17] Agogino A, Goebel K. BEST lab, UC Berkeley. Milling Data Set. NASA Ames Prognostics Data Repository, NASA Ames Research Center, Moffett Field, CA, 2007.